

## Video Article

# Analysis of Nephron Composition and Function in the Adult Zebrafish Kidney

Kristen K. McCampbell<sup>1</sup>, Kristin N. Springer<sup>1</sup>, Rebecca A. Wingert<sup>1</sup><sup>1</sup>Department of Biological Sciences, University of Notre DameCorrespondence to: Rebecca A. Wingert at [rwingert@nd.edu](mailto:rwingert@nd.edu)URL: <http://www.jove.com/video/51644>DOI: [doi:10.3791/51644](https://doi.org/10.3791/51644)

Keywords: Cellular Biology, Issue 90, zebrafish; kidney; nephron; nephrology; renal; regeneration; proximal tubule; distal tubule; segment; mesonephros; physiology; acute kidney injury (AKI)

Date Published: 8/9/2014

Citation: McCampbell, K.K., Springer, K.N., Wingert, R.A. Analysis of Nephron Composition and Function in the Adult Zebrafish Kidney. *J. Vis. Exp.* (90), e51644, doi:10.3791/51644 (2014).

## Abstract

The zebrafish model has emerged as a relevant system to study kidney development, regeneration and disease. Both the embryonic and adult zebrafish kidneys are composed of functional units known as nephrons, which are highly conserved with other vertebrates, including mammals. Research in zebrafish has recently demonstrated that two distinctive phenomena transpire after adult nephrons incur damage: first, there is robust regeneration within existing nephrons that replaces the destroyed tubule epithelial cells; second, entirely new nephrons are produced from renal progenitors in a process known as neonephrogenesis. In contrast, humans and other mammals seem to have only a limited ability for nephron epithelial regeneration. To date, the mechanisms responsible for these kidney regeneration phenomena remain poorly understood. Since adult zebrafish kidneys undergo both nephron epithelial regeneration and neonephrogenesis, they provide an outstanding experimental paradigm to study these events. Further, there is a wide range of genetic and pharmacological tools available in the zebrafish model that can be used to delineate the cellular and molecular mechanisms that regulate renal regeneration. One essential aspect of such research is the evaluation of nephron structure and function. This protocol describes a set of labeling techniques that can be used to gauge renal composition and test nephron functionality in the adult zebrafish kidney. Thus, these methods are widely applicable to the future phenotypic characterization of adult zebrafish kidney injury paradigms, which include but are not limited to, nephrotoxicant exposure regimes or genetic methods of targeted cell death such as the nitroreductase mediated cell ablation technique. Further, these methods could be used to study genetic perturbations in adult kidney formation and could also be applied to assess renal status during chronic disease modeling.

## Video Link

The video component of this article can be found at <http://www.jove.com/video/51644/>

## Introduction

The kidney is a complex organ that fulfills a multitude of physiological functions in the body. The foremost function of the kidney is metabolic waste excretion, and this task is closely intertwined with the maintenance of fluid homeostasis. The kidney performs these jobs by filtering the blood and forming urine, while concomitantly regulating blood pressure, electrolyte levels, and acid-base balance. Highly specialized epithelial tubules called nephrons serve as the basic functional unit of the kidney<sup>1,2</sup>. In adult vertebrates, nephrons are typically organized in a tightly coiled arrangement surrounding a centralized drainage system, thus allowing for many tubules to pack into the fairly small organ. For example, each human kidney can contain over 1 million nephrons<sup>3</sup>. Other mammals like the mouse possess on the order of 8-10 thousand nephrons per kidney<sup>4</sup>. The degree of renal complexity differs between these mammals and other vertebrates due to variations in total nephron number and their architectural layout within the kidney. Vertebrate species form as many as three successive kidney structures during development, and each form displays increasing complexity with regard to nephron endowment and arrangement: the pronephros, mesonephros, and metanephros. The last renal structure to be retained serves as the adult kidney organ—typically a mesonephros or a metanephros<sup>2</sup>. Each kidney form, however, has a nephron-based composition<sup>2</sup>.

The nephron is the workhorse of the kidney and is responsible for blood filtration along with metabolite secretion and reabsorption. Nephrons are simple tubular structures comprised of epithelial cells and have a segmental organization, in which discrete, highly specialized domains of differentiated epithelia perform specific tasks. In the order of filtrate flow through the nephron, there are typically three major parts that comprise each unit: (1) the renal corpuscle, (2) a tubule with proximal, intermediate, and distal segments, and (3) a collecting duct<sup>1</sup>. The proximal tubule is responsible for the reabsorption of organic solutes, most notably glucose and amino acids<sup>1</sup>. The intermediate tubule (or loop of Henle) is a major site of salt and water regulation<sup>1</sup>. Finally, fine-tuning of salt and other ions occurs in the distal tubule and collecting duct and is highly regulated by the endocrine system<sup>1</sup>. From there, the filtrate travels through the ureter and bladder, ultimately exiting the body as a waste product<sup>1</sup>.

The loss of renal function can stem from a multitude of causes that prevent normal nephron activity. These causes can occur during kidney development, e.g., congenital defects that lead to the malformation of nephrons<sup>5</sup>, or causes from different types of injury (stemming from both genetic and environmental origins). Acquired injuries are broadly categorized as acute kidney injury (AKI) or chronic kidney injury (CKD). AKI involves an abrupt loss of renal function, often resulting from ischemia or toxin exposure<sup>6,7</sup>. In mammals, nephron epithelial repair is possible after such injuries<sup>8</sup>, and many people exhibit full restoration of renal function after AKI. However, AKI is also associated with high morbidity and mortality that have been reported across a broad 30 - 70% incidence range<sup>6,7</sup>. CKD, in contrast, is associated with progressive loss of renal

function that results from years of prolonged damage, typically associated with fibrosis<sup>8,9</sup>. Further, an interplay exists between AKI and CKD, as either one can predispose an individual to the other<sup>10-12</sup>. For instance, those who have suffered from AKI are more susceptible to CKD and even death<sup>13</sup>. The incidence of kidney disease, both in the US and worldwide, has reached epidemic proportions and is predicted to rise as the aged population expands—thus there is a growing need to identify regenerative medicine interventions for the kidney<sup>14,15</sup>.

Despite the knowledge that AKI patients can recover, it has long been thought that the kidney is an organ without innate regenerative powers. This traditional view has been dramatically revised in recent years<sup>16</sup>. Studies investigating renal damage in mice and rats after AKI have shown that nephron tubule epithelial cells can proliferate and rebuild functional nephrons<sup>17-20</sup>. Although mammals possess this adaptive ability to regenerate nephrons, there are notable limitations and maladaptive responses can be triggered which lead to renal fibrosis and CKD<sup>21</sup>. For example, a recent study demonstrated that repeated epithelial cell ablation in murine nephrons was associated with diminished regeneration and renal fibrosis—suggesting nephrons have a limited regeneration threshold<sup>22</sup>. There is no evidence that the adult mammalian kidney forms new nephrons to replace lost or damaged ones, thus their destruction leads to a permanent nephron deficit<sup>8,9</sup>. Interestingly, some vertebrates do respond to AKI by regenerating nephron epithelia and by also producing new nephrons, a process referred to as neonephrogenesis or nephron neogenesis<sup>23</sup>. Neonephrogenesis occurs in fish after toxin exposure or partial resection, and injury models have historically included the goldfish<sup>24,25</sup>, tilapia<sup>26</sup>, skate<sup>27</sup>, medaka<sup>28</sup>, and more recently, the zebrafish<sup>29,30</sup>. Of these, zebrafish provide a viable genetic research model to discover the cellular and molecular pathways responsible for renal regeneration.

In this video article, we demonstrate how to label nephron segments in adult zebrafish. Knowledge of nephron anatomy, molecular features, and functional characteristics are essential for successful future renal studies using zebrafish. The adult zebrafish kidney is a mesonephros structure and is inherently less complex in terms of nephron number and organization than the metanephros structure found in adult mammals, avians, and reptiles<sup>31</sup>. However, zebrafish nephron segment organization is analogous to mammals, and was first documented in the embryonic kidney based on gene expression studies<sup>31-35</sup>. Zebrafish embryo nephrons contain linear tubule segments that include the proximal convoluted tubule (PCT), proximal straight tubule (PST), distal early (DE), and distal late (DL)<sup>31-35</sup> (**Figure 1**). Zebrafish adult nephrons possess similar tubular segments<sup>30,31,36,37</sup> (**Figure 1**). The PCT can also be identified by a functional phenotype: epithelial cells in the PCT will incorporate fluorescently labeled dextran compounds (10-70 kDa in size) present in the circulation, which has been used in both the embryonic and adult zebrafish kidney to assess endocytic uptake by these proximal tubule cells<sup>38-41</sup> (**Figure 1**). One difference in nephron segments between zebrafish and mammals is that zebrafish lack an intermediate tubule, or loop of Henle<sup>30-37</sup>; since this segment functions in mammals to conserve water, and zebrafish are a freshwater species without an urgency to concentrate their urine, it is not surprising that zebrafish lack this segment<sup>32,33</sup>. Thus, the overall nephron composition is largely conserved between the zebrafish and mammalian kidney<sup>32,33</sup>. These similarities have enabled zebrafish to be an effective research tool to investigate the functions of renal-expressed genes during developmental nephrogenesis<sup>32-35,42</sup> and to model numerous kidney diseases<sup>43,44</sup>, thereby adding to the substantial list of human conditions that can be investigated using zebrafish<sup>45,46</sup>.

Today, the adult zebrafish kidney is an attractive model for comparative studies of renal regeneration due to its genetic tractability and the expanding palate of technological resources available to interrogate gene function and signaling pathways in this species. Several studies have used the zebrafish mesonephros to investigate the mechanisms of regeneration after AKI<sup>29,30,37</sup>. For continued AKI research using the adult zebrafish kidney, it is essential to have exquisite methods to label different nephron regions and methods to survey nephron functionality. Several methods for adult kidney analysis have been adapted from embryonic kidney protocols. Intraperitoneal injection of fluorescently labeled dextran in the adult zebrafish labels the PCT epithelium in mesonephros nephrons via endocytosis<sup>30</sup>, as in zebrafish embryos<sup>38-41</sup> (**Figure 1**). This method has been used to visualize when proximal tubules regain their reabsorbing property following AKI, which enables one assessment of restored physiological function<sup>30</sup> (**Figure 1**). Another feature of the nephron proximal tubule is that the epithelial cells in this segment possess a brush border<sup>37</sup> that shows high levels of endogenous alkaline phosphatase activity. Thus, the proximal epithelium can be localized visually in the adult zebrafish kidney using a fluorescence-based technique known as ELF-(Enzyme-Labeled Fluorescence)-97<sup>47</sup>.

Here, we describe how to perform fluorescent dextran uptake assays<sup>30,48</sup> in the adult zebrafish kidney, so as to obtain a functional assessment of the proximal tubule and map the size and contours of this tubule segment. Next, we describe techniques to label the proximal tubule regions of the adult nephron with the fluorescent label alkaline phosphatase. Third, we show for the first time that the rhodamine-tagged lectin *Dolichos biflorus* agglutinin (DBA), which has been used as a general marker of the collecting ducts in the mammalian kidney<sup>49</sup>, marks the distal tubules of the adult zebrafish kidney. As DBA is mutually exclusive to alkaline phosphatase staining, these labels provide a way to broadly distinguish pan-proximal versus pan-distal stretches of the adult zebrafish nephron. Throughout the implementation of these fluorescent stains in both whole mount and cryostat histological sections, we correlate these labels with expression domains of solute transporter genes that uniquely identify each nephron segment. Therefore this protocol also contains a guide to the modified tissue processing procedures for adult tissue whole mount *in situ* hybridization (WISH) analysis based on our embryo WISH protocol<sup>50</sup>. These procedures can be used in various combinations (**Figure 2**) to document morphological and functional attributes of adult zebrafish kidney nephrons. Thus, these protocols can be applied to regeneration studies, the phenotypic characterization of other renal disease models, and even used to study formation of the adult kidney.

## Protocol

The procedures for working with zebrafish described in this protocol were approved by the Institutional Animal Care and Use Committee at the University of Notre Dame. Note: A guide to kidney and nephron anatomy in the zebrafish is provided (**Figure 1**). An overview of the methodologies described in this protocol is provided as a flow chart (**Figure 2**) to illustrate how multiple labeling procedures can be performed on the same kidney sample. For Part 7 on WISH preparation for adult kidney studies, the steps provided here indicate how to modify the processing of zebrafish embryos, as recently published<sup>50</sup>, to provide a technical guide for successful WISH analysis of the kidney organ.

### 1. Adult Zebrafish Intraperitoneal Injection with Dextran of Interest

1. Prepare the desired fluorescently labeled dextran stock(s) by dissolving the dextran powder in distilled water at a concentration of 50 mg/ml, then store aliquots in microcentrifuge tubes at -20 °C in the dark. Note: Various fluorescently labeled dextrans are commercially available. Select the dextran for use based on the combination of other labels that are desired, and make sure the appropriate fluorescent filters are

available with the microscopes that will be utilized. Lysine-fixable dextrans show fluorescence without any further labeling steps in living samples, unfixed tissue sample from euthanized specimens, and fixed specimens.

2. Thaw the desired dextran stock and store on ice in the dark while performing steps 1.3-1.5. Wrap the microcentrifuge tube in aluminum foil to protect it from light while handling.
3. Anesthetize an adult zebrafish between 5-7 months in age by placing the fish into a dish containing either 0.02% tricaine or 0.001% 2-phenoxyethanol for approximately 1 - 2 min. Note: It is preferable to use adult zebrafish of this age range because younger fish can have small kidneys that are difficult to dissect, and kidney samples from old fish can contain masses of scar tissue that cannot be analyzed. When properly anesthetized, the adult zebrafish will not exhibit a response to touch stimulation, which can be tested by using a spoon or blunt probe to gently touch the caudal fin of the fish.
4. Using a plastic spoon, lift the fish from the dish, decant the solution and carefully place the animal on a wet sponge mold, ventral side up.
5. Using a 31 G 1.0 cc insulin syringe, inject 20  $\mu$ l of thawed dextran stock solution into the intraperitoneal space. Orient the needle so that insertion occurs at a shallow angle at the ventral midline of the abdomen. To avoid puncturing organs, insert the needle then slightly raise it so as to lift the body wall of the fish and create a space in which to inject the dextran solution<sup>48</sup>. Note: Alternatively, the dextran stock can be diluted, e.g., at a ratio of 1:2 or 2:1 (dextran:distilled water), to reduce background fluorescence in the sample.
6. Gently return the fish to the tank to allow recovery from anesthesia. Note: Uptake of dextran by the proximal tubule segment occurs within 8 - 12 hr and can be detected for at least up to 3 days post-injection (dpi). Analysis at 3 dpi provides strong tubule signal with low background fluorescence in the renal stromal populations. Proceed to Part 2 for whole mount examination of dextran uptake alone, if additional labeling is not desired. For combinatorial labeling, proceed to Part 3 to prepare the tissue for whole mount examination of dextran uptake, then Part 4 to double-label with alkaline phosphatase and/or Part 5, to perform DBA double- or triple-labeling. For research using histological sections, proceed to Part 6 for instructions regarding how to make fine sections of the kidney using a cryostat and how to stain these with various labels and/or immunohistochemistry with primary and secondary antibodies.

## 2. Dissection and Flat Mount Preparation of the Adult Zebrafish Kidney from an Unfixed Animal Sample to Visualize Fluorescent Dextran Labeling of the Proximal Tubule

1. Euthanize the dextran-injected adult zebrafish by placing it into a dish with 0.2% Tricaine pH 7.0 for 4 - 5 min. Note: Ensure that the fish has been euthanized before proceeding, by monitoring carefully whether the gills have ceased movement and the heart has stopped beating<sup>36</sup>.
2. Using a plastic spoon, lift the fish from the Tricaine solution, decant the solution and place the animal on a tissue or paper towel.
3. Use a sharp pair of dissection scissors to make a cut behind the gill operculum and remove the head.
4. Immediately open the body of the fish with the dissection scissors by making a long ventral incision from the head to the base of the caudal fin.
5. Remove the internal organs of the fish using a pair of fine forceps.
6. Use super-fine dissection needles to pin open the body walls so as to allow visualization of the kidney organ, which is adherent to the dorsal wall of the animal.
7. Use fine forceps to detach the kidney from the dorsal wall.
8. Gently place the kidney into a 5 ml glass vial containing 1X PBS and wash 3 times with 3 - 5 ml of fresh 1X PBS for 5 min each. Note: The use of a glass vial for handling of adult kidney samples facilitates visualization of the tissue and allows for washes with large volumes (relative to the tissue mass) of approximately 3 - 5 ml. Alternatively, a 12-well cell culture dish can be used. While a plastic microcentrifuge tube could be used, the standard sized tubes (1.5 ml) could restrict the washing.
9. Remove the kidney with a transfer pipet and place onto a clean glass slide with 1-2 drops of 1X PBS.
10. Use fine forceps to flatten the kidney on the slide, making sure no tissue has curled or otherwise overturned on itself. Note: Alternatively, a tungsten wire tool can be used to make small incisions in the connective tissue to facilitate flat positioning of the kidney.
11. Place small pieces of modeling clay on each corner of an 18 x 18 mm glass coverslip and slowly set the coverslip onto the kidney. Note: Slightly angle the coverslip during placement to minimize trapping air bubbles in the solution<sup>50</sup>. The modeling clay divots are approximately 2 mm in diameter (**Figure 2A**). Alternatively, divots of vacuum grease can be substituted in lieu of modeling clay. Add an additional drop of 1X PBS to fill the space between the coverslip and glass slide if necessary.
12. Observe and/or image the kidney by placing the glass slide into the field of view on a stereomicroscope or compound microscope with the appropriate filter. Note: Refer to **Figure 2A** for macroscopic appearance of this slide preparation.

## 3. Fixation, Dissection, Permeabilization and Removal of Pigmentation of the Adult Zebrafish Kidney

1. Prepare a fresh fixative solution of 4% paraformaldehyde (PFA)/ 1X PBS / 0.1% DMSO or thaw a frozen aliquot of 4% PFA/1 X PBS and add 0.1% DMSO. Caution: PFA is toxic and PFA solutions should be handled at a chemical hood while wearing suitable personal protective equipment, including gloves and a lab coat. In addition, PFA powder should be handled with care when making the stock solution.
2. Fill a dissection tray with enough fixative solution to submerge the entire animal.
3. Euthanize and mount the selected zebrafish in fixation solution (refer to Steps 2.2-2.6). Note: The selected fish can be an untreated zebrafish kidney specimen, or a kidney isolated from a zebrafish that previously received an intraperitoneal dextran injection (Part 1).
4. Fix the sample O/N (12 - 16 hr) at 4 °C.
5. The following day, use fine forceps to carefully detach the kidney from the dorsal body wall and place the organ into a glass vial using a transfer pipet. Note: Alternatively, a 12-well or 24-well culture dish can be used. While a plastic microcentrifuge tube could be used, the standard sized tubes (1.5 ml) could restrict the washing.
6. Wash the dissected kidney 3 times with 3 - 5 ml of 1X PBS with 0.05% Tween for 5 min each.
7. Remove the 1X PBS with 0.05 % Tween and rinse the kidney with 3 ml of a 5% sucrose solution (in 1X PBS) for 30 min.
8. Replace with 3 ml of 30% sucrose solution (in 1X PBS) and store O/N (12 - 16 hr) at 4 °C. Note: The sucrose solutions permeabilize the cellular membranes, subsequently allowing specific labeling of reagents as they penetrate the tissue.
9. The following day, remove the 30% sucrose solution and wash the kidney 2 times with 5 ml of 1X PBS with 0.05% Tween for 5 min each.

10. Replace the 1X PBS with 0.05% Tween with 3 - 5 ml of bleaching solution to remove the melanocyte pigmentation present on the kidney organ.
11. Place glass vial on a rotator and watch carefully as pigmentation disappears. Note: Depigmentation typically takes approximately 20 min when performed after sucrose treatment, but occasionally can take as long as 60 min. If the bleaching solution is left on the kidney for too long, disintegration of the organ can occur; it is advised to monitor the sample every 10-15 min to check tissue integrity.
12. When the pigmentation has been removed from the kidney, wash twice with 3 - 5 ml of 1X PBS with 0.05% Tween.
13. Replace the 1X PBS with 0.05% Tween with 3 - 5 ml of 4% PFA solution for 1 hr at RT.
14. Remove the 4% PFA solution and wash the kidney 3 times with 3 - 5 ml of 1X PBS with 0.05% Tween for 5 min each. Note: Once fixation is complete, the kidney also can be mounted on a glass slide and evaluated for dextran uptake sans the melanocyte pigmentation, by performing Steps 2.8-2.12.
15. Remove the 1X PBS with 0.05% Tween and replace with 3 - 5 ml of blocking solution, then incubate the kidney at RT in the block for 2 hr.
16. When blocking is complete, proceed directly to the selected staining protocol. Note: The kidney can now be processed through one or more other procedures in order to conduct labeling studies with different reagents. For whole mount labeling of the proximal tubule with only alkaline phosphatase, proceed to Section 4. For whole mount labeling of only the distal tubule go to Section 5. Alternatively, Sections 4 and 5 can be performed in linear succession for dual detection in whole mount.

#### 4. Labeling the Adult Kidney Proximal Tubule Segments with Alkaline Phosphatase Detection

1. Remove the block and wash the kidney 3 times with 3 - 5 ml of 1X PBS with 0.05% Tween for 5 min each, and then replace the 1X PBS with 0.05% Tween with 3 - 5 ml of 1X PBS. Let the kidney soak for at least 10 min. Note: During this time, transfer the kidney to a 12-well or 24-well culture dish if the tissue has been kept in a glass vial for previous processing steps.
2. Replace the 1X PBS with the sufficient working alkaline phosphatase substrate solution (Refer to detection kit located in the Table of Materials) to cover the sample, then place the sample on a rotator for 30 min at RT. Keep the sample protected from light.
3. Stop the reaction by washing the kidney in alkaline phosphatase wash buffer solution.
4. Rinse the kidney with 3 changes of wash buffer solution over 10 - 15 min. Note: After this step, proceed directly to Part 5, Step 5.1 (thus temporarily omitting Steps 4.5-4.6) if labeling with DBA is also desired. Optional step: To label and visualize cell nuclei in the organ, soak the kidney in propidium iodide solution. Prepare a propidium iodide stock by dissolving the powder at a concentration of 1 mg/ml (1.5 mM) in distilled water. Dilute the stock to 500 nM in 2X SSC and incubate the kidney in this solution for 30 min. Rinse with 1X PBS and proceed to Step 4.5.
5. Remove the wash buffer solution and mount the kidney onto a clean glass slide in the phosphatase mounting medium included in the labeling kit (Refer to Steps 2.9-2.12). Note: The mounting medium has replaced the 1X PBS from step 2.9.
6. Visualize the alkaline phosphatase stained kidney using a stereomicroscope or compound microscope with a Hoechst/DAPI filter set. Note: Optional step: Visualize the propidium iodide using a tetramethyl-rhodamine (TRITC) or Texas red filter.

#### 5. Demarcating the Adult Kidney Distal Tubule Segments with Rhodamine DBA

1. Prepare a 200  $\mu$ l working DBA solution by diluting DBA (2 mg/ml) 1:100 in 1X PBS.
2. Replace the 1X PBS with 0.05% Tween solution with the 200  $\mu$ l DBA solution.
3. Place on rotator for 1 hr at RT.
4. Remove the DBA solution and wash the kidney 3 times with 3 - 5 ml of 1X PBS for 5 min each. Note: Optional step: To label and visualize cell nuclei in the organ along with the DBA label, soak the kidney in DAPI solution to detect with a Hoechst/DAPI filter (rhodamine DBA stain can be detected with a TRITC or Texas red filter). Prepare a DAPI stock by dissolving powder at a concentration of 5 mg/ml (14.3 mM). Dilute the stock to 300 nM in 2X SSC and incubate the kidney in this solution for 20 min. Rinse with 1X PBS and proceed to step 5.5. If Part 4 processing has been performed, keep in mind that DAPI and alkaline phosphatase are both detected with a Hoechst/DAPI filter.
5. Remove the 1X PBS and mount the kidney on a clean glass slide (refer to Steps 2.9-2.12).
6. Visualize the DBA-stained distal segments of the kidney using a standard TRITC or Texas red filter set on a fluorescent stereomicroscope or compound microscope. Note: Optional step: Visualize the DAPI using a Hoechst/DAPI filter.

#### 6. Embedding, Cryosectioning and Staining (Vital Dyes and Immunohistochemistry Labeling) of Adult Zebrafish Kidney Tissue

1. Select fish for analysis, then euthanize, fix, and permeabilize as described (Steps 3.2-3.8). Note: Fix adult fish in 9:1 ethanol:formaldehyde/ 0.1% DMSO in lieu of 4% paraformaldehyde/ 1X PBS / 0.1% DMSO for the cryosection procedure to produce sections for dextran, alkaline phosphatase, and DBA visualization. However, keep in mind that paraformaldehyde-based fixations can be compatible for some immunohistochemistry procedures. Further, bleaching of the adult kidney is not needed for cryosection analysis, because the melanocytes are superficial and do not affect visualization of nephron cells that comprise the "inside" of the kidney organ.
2. The following day, remove the 30% sucrose solution and replace with 1:1 tissue freezing medium: 30% sucrose for 4 hr at RT.
3. Remove the 1:1 solution and embed kidney samples in 100% tissue freezing medium in cryomolds and place at -80 °C for at least 1 hr.
4. Transversely cut serial sections, approximately 12  $\mu$ m thick, through the entire adult kidney.
5. Mount frozen cryosections onto adhesive microscope slides and allow to air dry for 1 hr at 50 °C.
6. Store slides at -80 °C until use.
7. When cryosections are ready to be labeled, remove the microscope slides from -80 °C and place on slide warmer at 50 °C for 45 min.
8. Using a liquid blocker pen, draw a circle around the cryosections and let dry for 15 min on the slide warmer at 50 °C.
9. Remove slides from the slide warmer and place flat in a humidity chamber at RT.
10. Rehydrate the cryosections by adding 1X PBS with 0.05% Tween to the encircled portion of the slides for 20 min. Note: Approximately 200 - 300  $\mu$ l is needed to cover each encircled portion on a slide.

11. Replace the 1X PBS with 0.05% Tween solution with fresh 1X PBS and incubate for 10 min.
12. Remove 1X PBS and incubate cryosections in a blocking solution for 2 hr. Note: For a 10 ml blocking solution, combine 8 ml 1X PBS with 0.05% Tween, 2 ml fetal calf serum and 150  $\mu$ l DMSO. To perform immunohistochemistry after the blocking step, incubate the slide with the desired primary antibody diluted in fresh block O/N at 4 °C, wash once using 1X PBS with 0.05% Tween, incubate for 2 hr at RT with secondary antibody solution diluted in 1X PBS with 0.05% Tween, wash once using 1X PBS with 0.05 % Tween, and mount a coverslip on the slide with mounting medium. The required antibody dilutions will vary and trials should be performed to select the optimal dilutions. Antigen retrieval can also facilitate immunolabeling, and is performed before blocking. Immediately after slides are thawed at 50 °C (Step 6.8) incubate the cryosections between 95 °C-100 °C for 40 min in preheated 10 mM sodium citrate buffer. Cool the slides for 30 min, then wash twice in 1X PBS with 0.05% Tween, and proceed to Step 6.11.
13. Remove the blocking solution and wash cryosections 3 times with 1X PBS for 5 min each.
14. Replace 1X PBS with DBA staining solution and incubate for 1 hr. Note: Dilute 1  $\mu$ l DBA in 99  $\mu$ l of 1X PBS to make a 100  $\mu$ l staining solution.
15. Remove the DBA staining solution and wash cryosections 3 times with 1X PBS for 5 min each.
16. Apply alkaline phosphatase label and incubate on cryosections for 10 min.
17. Wash alkaline phosphatase off the cryosections with a series of 3 washes of wash buffer for 10 min each. Note: For a 100 ml solution of washing buffer, combine 5 ml of 0.5 M EDTA and 120 mg of levamisole into 95 ml of 1X PBS. To label nuclei, incubate the sections with propidium iodide or DAPI at the dilutions previously noted (Steps 4.4, 5.4, respectively) for 30 min at RT. Select a nuclear stain compatible with the combination of other fluorescent stains that have been chosen.
18. Remove all liquid from the cryosections and place 2 drops of mounting medium on microscope slide.
19. Carefully place micro cover glass onto the microscope slide. Cryosections are now ready to image with the appropriate filter(s).

## 7. WISH Processing for Adult Zebrafish Kidney Samples

1. Select the desired zebrafish specimen(s), euthanize, fix and dissect the kidney as described (Steps 3.1-3.5). Note: It is essential to use a fixative solution of 4% paraformaldehyde (PFA)/ 1X PBS with 0.1% DMSO to permeabilize the kidney. Place the kidney into a glass vial for easy visualization during subsequent processing steps.
2. Remove the fixative and wash the kidney twice with 5 ml of 1X PBST.
3. Remove the 1X PBS and wash the kidney twice with 100% methanol, then incubate the kidney at -20 °C for at least 20 min to permeabilize. Note: Dissected kidneys can be stored indefinitely -20 °C.
4. Rehydrate the kidney by performing a series of 5 min washes with 3 - 5 ml of 50% methanol/1X PBST, 30% methanol/1X PBST, and twice with 1X PBST.
5. Bleach the kidney to remove pigmentation as described (Steps 3.10-3.14).
6. Treat the kidney with 10  $\mu$ g/ml proteinase K/1X PBST with 0.1% DMSO for 20 min, then rinse twice with 1X PBST and post-fix in 4% PFA/1X PBST for 20 min to O/N. Note: Always prepare the proteinase K working solution immediately before sample digestion by combining 50  $\mu$ l of freshly thawed proteinase K stock (10 mg/ml), 50 ml of 1X PBST, and 50  $\mu$ l of DMSO.
7. Process the kidney for single or double WISH following the steps for riboprobe synthesis, prehybridization, hybridization, anti-digoxygenin/ anti-fluorescein antibody incubation and detection as recently described<sup>49</sup>. Note: Whole mount imaging of kidney stains should be performed within several days of performing the staining reaction. Nephron stains tend to fade very quickly, especially red substrate labels. For nephron photography, flat mount the kidney sample as described above in Steps 2.10 to 2.12, and image using a stereo- or compound microscope. Differential interference contrast filters can be employed to better visualize the cellular outlines of nephrons to facilitate sample analysis.

## Representative Results

Each of the protocols was performed on wild type zebrafish. Examples of the data obtained document the normal structural composition and properties of the nephrons within the healthy adult zebrafish kidney. The adult zebrafish possesses a mesonephros, or second kidney form that is located on the dorsal body wall (**Figure 1A**). The adult kidney is relatively flat and contains a so-called head, trunk, and tail region with superficial melanocytes scattered throughout these regions (**Figure 1A**). The renal tissue contains branched arrays of nephrons that connect and drain into central collecting ducts (**Figure 1A**). Each nephron is polarized along its length, with a blood filter (or renal corpuscle) at one end, followed by a series of tubule segments, and lastly terminating at a duct that collects the solution that will be excreted (**Figure 1A**). Each adult nephron tubule contains proximal and distal segments of cells, demarcated by the expression of specific solute transporters<sup>30,31,36,37</sup>, which is conserved with the segmental pattern exhibited by embryonic nephrons<sup>31-35</sup> (**Figure 1B**). For example, *cubilin* transcripts mark the proximal tubule<sup>39</sup> (PCT and PST) and *clcnk* transcripts mark the distal tubule<sup>32</sup> (DE and DL) (**Figure 1B**). Further, the PCT segment is distinguished by expression of *slc20a1a*, the PST is distinguished by expression of *slc13a1*, the DE is distinguished by expression of *slc12a1*, and the DL is distinguished by expression of *slc12a3*<sup>32</sup> (**Figure 1B**). Differences between adult nephron tubules compared to embryonic ones are that distal segments display convolutions (DE, DL) and the DL segment branches extensively in the adult, which is distinct from the linear, non-branched anatomy of these regions in the embryo<sup>30,31,36,37</sup> (**Figure 1A**). In both adult<sup>30</sup> and embryonic<sup>38-41</sup> nephron tubules, the PCT epithelium can be distinguished due to its endocytic properties and can be visualized and assessed for reabsorptive function based on the ability to uptake fluorescent dextran conjugates (**Figure 1B**). Further, as demonstrated in the subsequent figures, the adult proximal tubule (PCT and PST, or pan-proximal region) is labeled by alkaline phosphatase, while the distal tubule (DE and DL, or the pan-distal region) is labeled by DBA (**Figure 1B**). The methods used herein to label adult zebrafish nephron segments using dextran uptake, alkaline phosphatase, DBA, immunohistochemistry or WISH can be performed in various combinations, in whole mount or with histological sections of renal tissue (**Figure 2**). This allows for great flexibility and variety when nephron composition is to be assessed (**Figure 2**).

The adult kidney can be mounted flat on a glass slide for analysis, with divots of modeling clay (or alternatively, vacuum grease) used to suspend the coverslip over the tissue (**Figure 3A**). As the typical kidney length is approximately 5-7 mm, it has a size conducive to imaging on a stereo or compound microscope (**Figure 3A**). Under brightfield lighting, a superficial population of melanocytes with black pigmentation can be visualized in association with the kidney tissue, and vasculature such as the aorta can be seen because the circulating erythrocytes have a red hue (**Figure 3B**). Following intraperitoneal injection of dextran-FITC, PCT domains located throughout the mesonephros were still labeled 3 days later, and imaged using a FITC filter on a fluorescent microscope (**Figure 3C**). While melanocytes partly obscure the visualization of

individual renal tubules (**Figure 3C'**), the melanocytes do not prevent quantification of nephron number or the evaluation of tubule diameter and length. Following intraperitoneal injection of dextran fluoro-ruby, bleaching of the fixed sample eliminated the melanocyte pigmentation, and PCT segments were observed with bright field lighting alone (**Figure 3D**). Lipid droplets from the abdominal body cavity can sometimes be seen in association with whole kidney organ preparations (**Figure 3A**). Individual PCT segments show convolutions, coils (**Figure 3D'**) but also can be characterized by relatively linear stretches (**Figure 3D''**).

Different dextran conjugates provided different levels of overall clarity in proximal tubule labeling. In particular, dextran-FITC or dextran fluoro-ruby led to crisp nephron labels with minimal background (**Figures 3C-D''**). Both the dextran cascade blue and lucifer yellow conjugates showed proximal tubule uptake in the adult kidney (**Figure 4A, 4B**). Interestingly, kidneys exposed to dextran cascade blue showed relatively specific PCT fluorescence with some background (**Figure 4A, 4A'**), while kidneys exposed to dextran lucifer yellow had labeled PCT segments but showed noticeable background signal, with non-specific fluorescent staining present throughout in the renal stroma, or the space between the nephrons (**Figure 4B, 4B'**). Finally, the use of dextran-fluoro ruby provided superior proximal tubule labeling, with minimal or no background even when viewed at a range of different magnifications (**Figure 4C, 4C'**). In all cases, the distinctive tubular pattern of dextran conjugate uptake correlated with the WISH expression of transcripts encoding *slc20a1a*, an established PCT-specific marker<sup>30-32</sup> (**Figure 4D**). Nephron PCT segments stained with *slc20a1a* antisense riboprobe displayed S-shaped PCT coils, as well as less sharply coiled PCT segments (**Figure 4D'**), as observed during labeled dextran conjugate assays (**Figure 3D', 3D''**).

Other kidney preparations, such as detection of the proximal tubule alkaline phosphatase activity (**Figure 5A, 5B, 5C**) were similarly performed after removal of the melanocyte pigmentation. This allowed for proximal tubule nephron imaging and analysis without any obstruction. Endogenous alkaline phosphatase reactivity in the nephron is one major hallmark of the proximal tubule<sup>1,47</sup>. Alkaline phosphatase staining is highly specific for proximal nephron regions, as compared to the pan-proximal WISH expression pattern of the gene *cubilin*<sup>39</sup> (**Figure 5D, 5D'**). Alkaline phosphatase reactivity was most intense in the first section of the proximal tubule that corresponds to the PCT (**Figure 5B**), similar to the pattern of *cubilin* expression (**Figure 5D, 5D'**), which also had highest relative transcript levels in the PCT. The PCT was distinguished by its slightly wider diameter, specific expression of the transcription factor *mafba* (**Figure 5E, 5E'**), and specific expression of the solute transporter gene *slc20a1a* (**Figure 4D, 4D'**). Alkaline phosphatase reactivity also labeled a stretch of proximal tubule with a thinner diameter that corresponds to the PST segment (**Figure 5B**) based on comparison to the segment-specific transcript expression of the solute transporter gene *slc13a1* (**Figure 5F, 5F'**). The WISH expression domains of the PCT marker *slc20a1a* and PST marker *slc13a1* are mutually exclusive (**Figure 5G**), and close examination of single nephrons showed that these respective domains abut, with little if any gap between them, and that together they recapitulate the expression domain of *cubilin* (black arrowheads in **Figure 5G', 5G'', 5G'''**).

To further confirm the relationship of alkaline phosphatase reactivity with proximal tubule identity, whole mount co-labeling of alkaline phosphatase staining was performed on kidneys from zebrafish that received an intraperitoneal injection of dextran fluoro-ruby 3 days prior (**Figure 6A-C**). Dextran fluoro-ruby showed overlap with alkaline phosphatase in just the wider-diameter portion of the proximal tubule domain that corresponds to the PCT (examples in **Figure 6D-I**). The dextran-positive domain abruptly stopped at the site where the diameter of the proximal tubule thinned, *i.e.*, where the PCT and PST met, (white arrowheads in **Figure 6**) and only alkaline phosphatase reactivity was observed in the subsequent PST segment (examples in **Figure 6D-I**). Background fluorescence from the alkaline phosphatase reaction also dimly outlined the pair of parallel major collecting duct tracks found in the adult kidney<sup>29,30</sup>—ducts which are distinguished by having the widest diameter of any renal-associated tube (asterisks in **Figure 6A, 6D, 6E, 6G, 6H**). Next, the co-labeling of nephron tubules with alkaline phosphatase and dextran uptake was observed in cryosection analysis (**Figure 6J**, tubule perimeters outlined with white dots). In cross-section, the alkaline phosphatase reactivity was noted in a thick band at the apical surface of the tubular epithelium, consistent with brush border ultrastructure, while the corresponding tubular cell cytosolic space showed dextran fluoro-ruby reactivity (**Figure 6J**). Notably, stained tubules were either double positive for alkaline phosphatase and dextran, leading to their identification as PCT segments, or singly positive for alkaline phosphatase (**Figure 6J**, tubule perimeter outlined in yellow dots), leading to an identification as a PST segment (note: other tubules present were negative for both stains, data not shown) (**Figure 6J**). Further, alkaline phosphatase staining (**Figure 6K**) was successfully combined with a nuclear label, propidium iodide (**Figure 6L**), facilitating cell counting (overlay in **Figure 6M**).

The distal tubule of the adult zebrafish nephron was labeled with rhodamine-conjugated DBA (**Figure 7**). Whole mount double-labeling with DBA and alkaline phosphatase was performed on kidneys from wildtype zebrafish (**Figure 7A-C**). DBA and alkaline phosphatase reactivity showed no overlap in nephron tubules (**Figure 7D-H**). DBA stained tubules showed a markedly thinner diameter compared to alkaline phosphatase positive tubules, and DBA tubules were often branched (white arrowheads, **Figure 7G, 7H, 7J**), whereas branching was never observed in tubule segments stained with alkaline phosphatase. Renal cryosections were collected from wildtype zebrafish that carry a transgene in which the *enpep* promoter drives eGFP (*Tg:enpep:eGFP*), as GFP labels both the proximal and distal nephron tubules<sup>51</sup> (**Figure 7I**). Immunohistochemistry was performed to detect GFP, so as to label all of the renal tubules (green, **Figure 7I**), followed by fluorescent labeling with alkaline phosphatase and DBA (turquoise and red, respectively, **Figure 7I**). Analysis of tubule sections revealed that tubules were either positive for alkaline phosphatase or DBA, but not both labels (**Figure 7I**). Only rare tubules showed reactivity with neither alkaline phosphatase nor DBA stain, possibly due to the angle of the tubule section (white arrow, **Figure 7I**). Further, DBA staining was successfully combined in whole mount kidney staining with the nuclear label DAPI (**Figure 7J**), again emphasizing the characteristic branched nature of the distal tubule segments (white arrowheads, **Figure 7J**).

Next, to further compare the patterns of dextran-FITC uptake, alkaline phosphatase, and DBA, triple labeling was examined by intraperitoneally injecting adult zebrafish with dextran-FITC, followed by kidney isolation 3 days later followed by cryosectioning and staining for alkaline phosphatase and DBA (examples provided in **Figure 8A-E**). Renal tubules showed three categories of label combinations: tubules that were double positive for alkaline phosphatase and dextran denoted PCT segments (white dotted lines), tubules positive for alkaline phosphatase alone denoted PST segments (yellow dotted lines), and distal tubules were labeled by just DBA (red dotted outlines **Figure 8A-E**). Further, only DBA positive tubules exhibited branch points (**Figure 8E**). By WISH analysis, this distinctive branching pattern of the distal, DBA positive tubules correlated with the gene expression patterns of solute transporter transcripts that are specific for distal tubule segments (**Figure 8F-I**). Transcripts encoding *clcnk*, which marks the entire distal tubule (DE and DL) were thin in diameter, plentiful in the kidney, and contained branch points (black arrowhead **Figure 8F, 8F'**). In comparison, tubule segments that showed expression of *slc12a1* or *slc12a3*, which are markers of the DE and DL, respectively, were less plentiful in kidney samples overall compared to *clcnk* expression (compare **Figure 8G and 8F, 8H**). Further, tubule segments that expressed *slc12a1* were rarely, if ever, branched (**Figure 8G, 8G'**), whereas tubule regions that expressed *slc12a3*

were frequently branched in characteristic pinwheel-like arrangements (**Figure 8H, 8H', 8H'', 8H'''**, black arrowheads). Finally, double WISH for the PCT marker *slc20a1a* and the distal marker *clcnk* showed that these stains were not overlapping (**Figure 8I**). Notably, the stretches of *slc20a1a*-expressing PCT segments were not attached to *clcnk*-expressing tubules, which was expected since the PST is situated between these regions (**Figure 8I**). Taken together, the assays of labeling renal tubules with dextran uptake, alkaline phosphatase reactivity, DBA, and WISH for specific gene transcripts, enables the discernment of proximal versus distal segments.

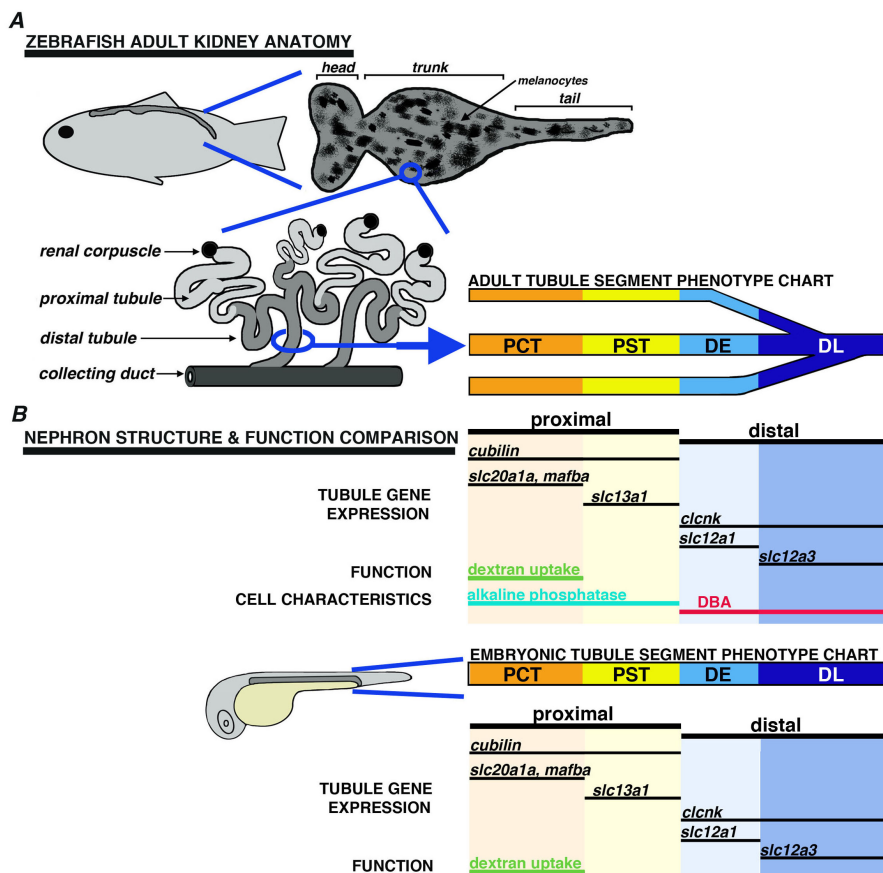


**Figure 1. Nephron anatomy in the adult zebrafish kidney.** Schematic drawings of the **(A)** adult zebrafish kidney and **(B)** a comparison chart of segment molecular characteristics exhibited by adult and embryonic zebrafish nephrons. **(A)** (Top left) The adult kidney is a flat organ located on the dorsal body wall. (Top right), When viewed from a ventral perspective, the kidney has a distinctive curved morphology, consisting of head, trunk and tail regions, and also has a surface population of associated melanocytes. Enlargement (bottom left) shows a schematic of a typical nephron tree in the adult zebrafish kidney, in which each single nephron possesses a blood filter (renal corpuscle) on one end, followed by a proximal tubule, distal tubule, and duct. Colored schematic (bottom right) shows a linear diagram of one adult nephron tree to compare segment characteristics with those of embryonic nephrons **(B)**. The zebrafish embryo nephrons contain tubule segments that include the proximal convoluted tubule (PCT), proximal straight tubule (PST), distal early (DE), and distal late (DL), with respective gene expression domains listed below. Nephrons in the adult zebrafish have a similar segmental composition and analogous molecular signature based on the expression domains of genes that encode solute transporters, although a notable distinction compared to the embryo is that several nephrons can be united through a branched DL segment. [Please click here to view a larger version of this figure.](#)

**NEPHRON SEGMENT LABELING METHODOLOGY FLOW CHART:  
WHOLE MOUNT AND HISTOLOGICAL SECTION PREPARATIONS**

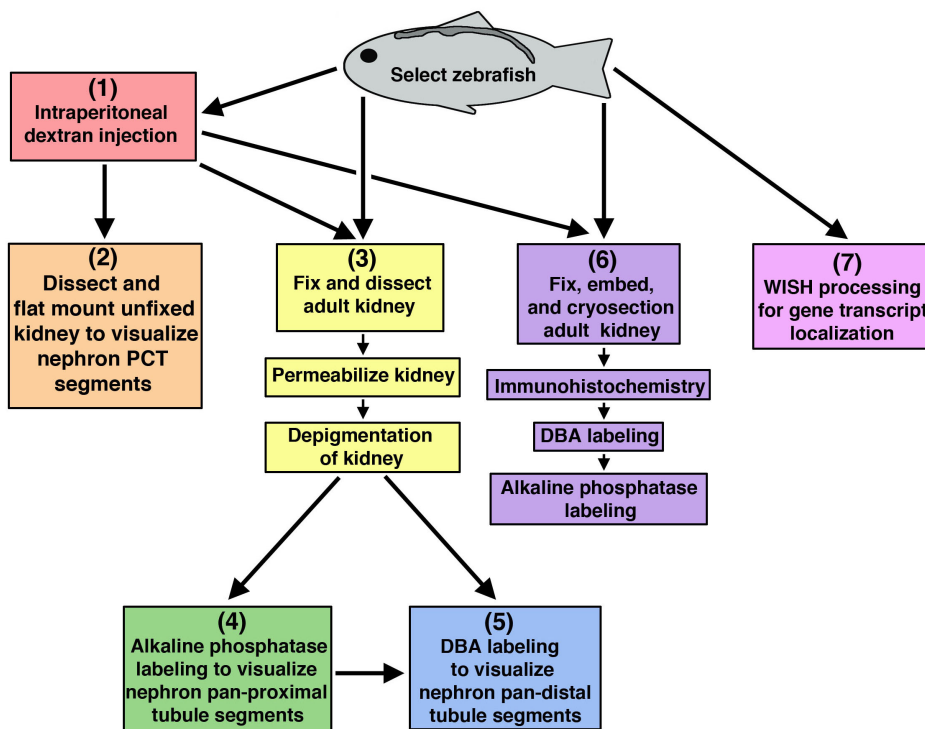


**Figure 2. Flowchart map indicating the relationship between the methods depicted in this protocol, indicating how the methods can be performed singly or in assorted combinations.** Following intraperitoneal injection of labeled lysine-fixable dextran into the adult zebrafish, the kidney can be visualized in a whole mount preparation, either alone or in combination with alkaline phosphatase and/or DBA stains. Alternatively, the selected zebrafish kidney can be examined after histological tissue sectioning with a cryostat. The sections can be stained to label numerous combinations of attributes, using immunohistochemistry, nuclear staining, DBA staining, and/or alkaline phosphatase reactivity. In addition, renal sections can be visualized directly for the presence of lysine-fixable dextran uptake in PCT segments. Finally, selected kidneys can be processed for the spatiotemporal expression of gene expression using WISH. Bracketed numbers refer to corresponding protocol parts. [Please click here to view a larger version of this figure.](#)

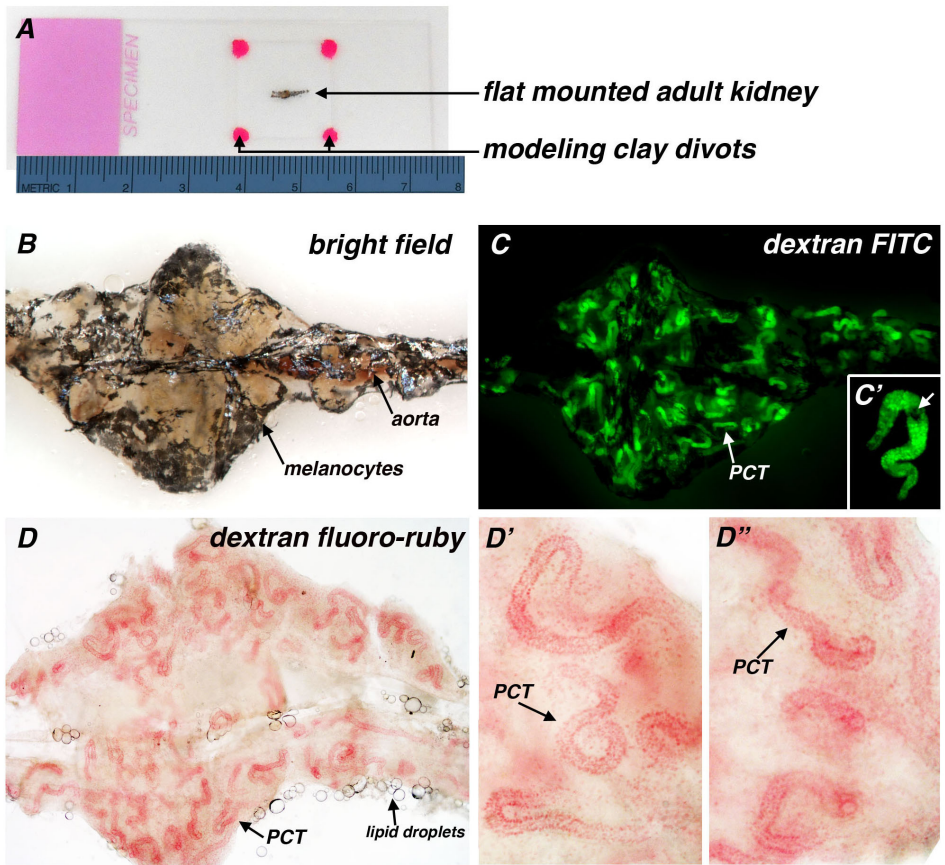


**Figure 3. Adult zebrafish kidney flat mount preparation and application to visualize conjugated dextran uptake in the PCT segment of kidney nephrons.** (A) Brightfield image of a kidney specimen flat mount preparation, in which the organ has been positioned flat on a glass slide, with a coverslip placed on top of the tissue that is resting on four divots of modeling clay (hot pink color). Here the renal preparation is imaged alongside a metric ruler to provide a scaled comparison. The typical adult kidney is approximately 5-7 millimeters (mm) from head to tail. (B) Brightfield image of an unbleached kidney. The black pigmentation corresponds to the scattered population of melanocytes found in association with the kidney, and the aorta runs along the midline of the kidney. (C) Visualization of nephron PCT segments 3 days following intraperitoneal injection of 40 kDa dextran-fluorescein (FITC), without bleaching of the adult kidney. PCT segments are seen throughout the kidney but are partly obscured due to the melanocytes. (C') Digital zoom of a single nephron, with melanocytes (white arrow). (D) Image of an adult kidney 3 days following intraperitoneal injection of 10 kDa dextran fluoro-ruby, fixation of the kidney, and bleaching. The melanocyte pigmentation was removed and the PCT regions were visualized here based on their endocytic uptake of dextran under brightfield lighting. Lipid droplets (arrow) from the abdomen can sometimes be seen in association with renal tissue samples. (D', D'') Representative images depict slight morphological variations between PCT segments. While many nephron PCTs are tightly coiled (D'), other nephrons contain PCT regions that have minimal coiling (D''). [Please click here to view a larger version of this figure.](#)

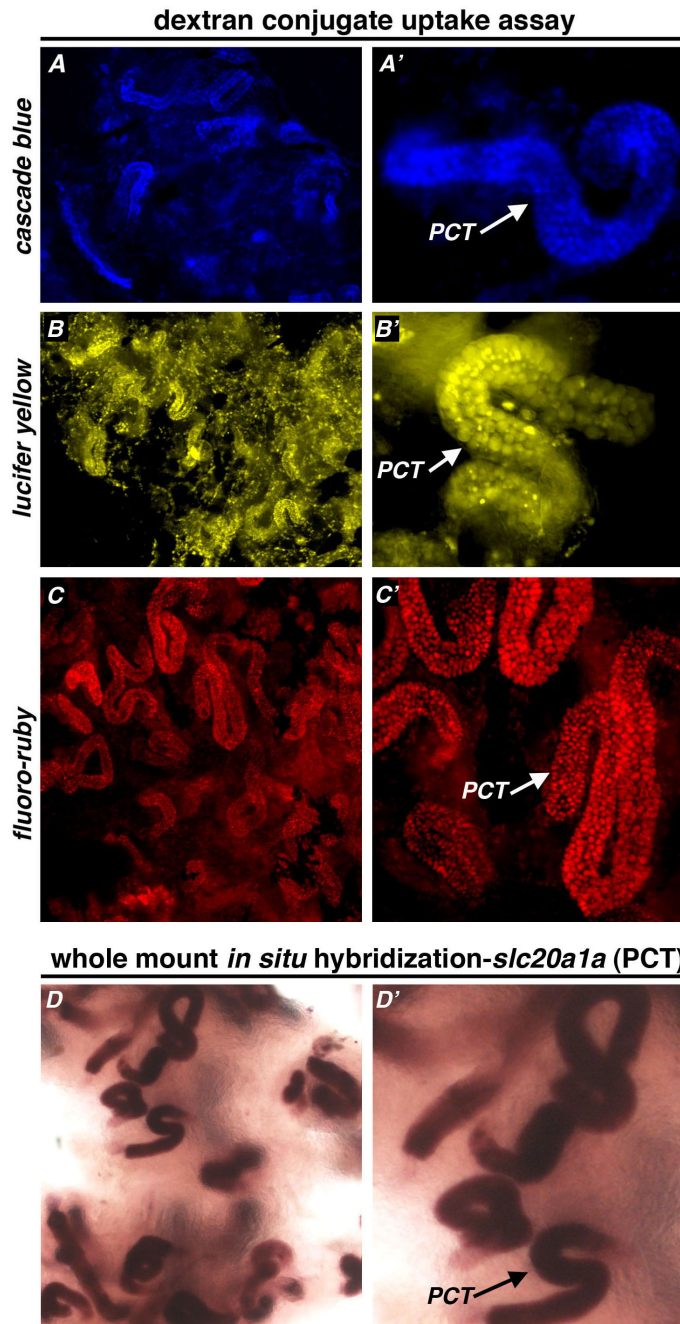


**Figure 4. Adult kidney nephron PCT tubule segment labeling.** Wildtype zebrafish were intraperitoneally injected with a single fluorescent dextran conjugate; then their kidney was examined 3 days after the injection for PCT visualization. **(A, A')** Dextran cascade blue, 10 kDa **(B, B')** dextran lucifer yellow, 10 kDa and **(C, C')** dextran fluoro-ruby, 10 kDa all preferentially label the PCT segments in renal nephrons. Both dextran cascade blue and lucifer yellow show some non-specific labeling of stromal cell populations located between nephrons, with much higher background observed in lucifer yellow treated kidneys. In contrast, dextran fluoro-ruby showed dramatically reduced background with intense PCT labeling. **(D, D')** An adult kidney stained by WISH to detect the location of transcripts encoding *slc20a1a*, a specific marker of the PCT transporter cell type. The expression domain of *slc20a1a* matches the characteristic pattern of dextran uptake observed in the kidney, with a distribution of various tightly coiled/looped PCT domains as well as more elongated PCT stretches that show a consistent wide diameter. [Please click here to view a larger version of this figure.](#)

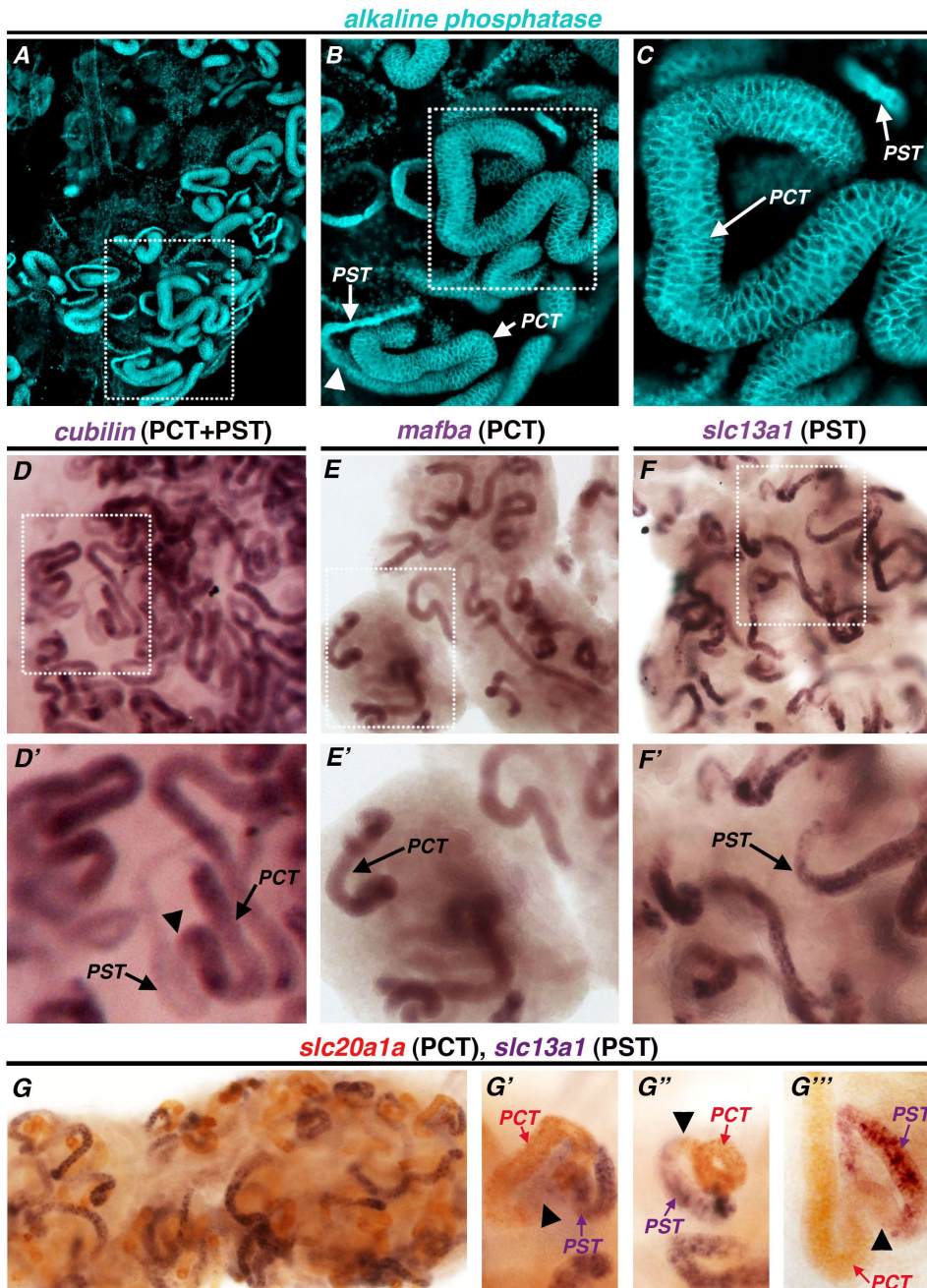


**Figure 5. Representative result of staining for alkaline phosphatase, a pan-proximal tubule marker, in the adult zebrafish kidney compared to other proximal tubule markers assessed with WISH. (A-C)** Alkaline phosphatase staining (turquoise) illuminates the nephron proximal tubule, highlighting both the PCT and PST. **(D-F')** Single WISH for the listed genes (each in purple staining). **(D, D')** The expression pattern of *cubilin*, a pan-proximal (PCT-PST) marker, correlates with alkaline phosphatase **(D, D')**. In comparison, WISH for *mafba* marks the PCT **(E, E')** and *slc13a1* marks the PST **(F, F')**. In **(G-G''')** double WISH for the PCT marker *slc20a1a* (red) and the PST marker *slc13a1* (purple) shows that the segments labeled by these markers do not overlap, and rather that their expression domains occupy adjacent positions when single nephrons are closely examined **(G'-G''')**. Black arrowheads indicate the junction between PCT and PST segments, which is typically associated with a change in tubule diameter from large to small, respectively. [Please click here to view a larger version of this figure.](#)

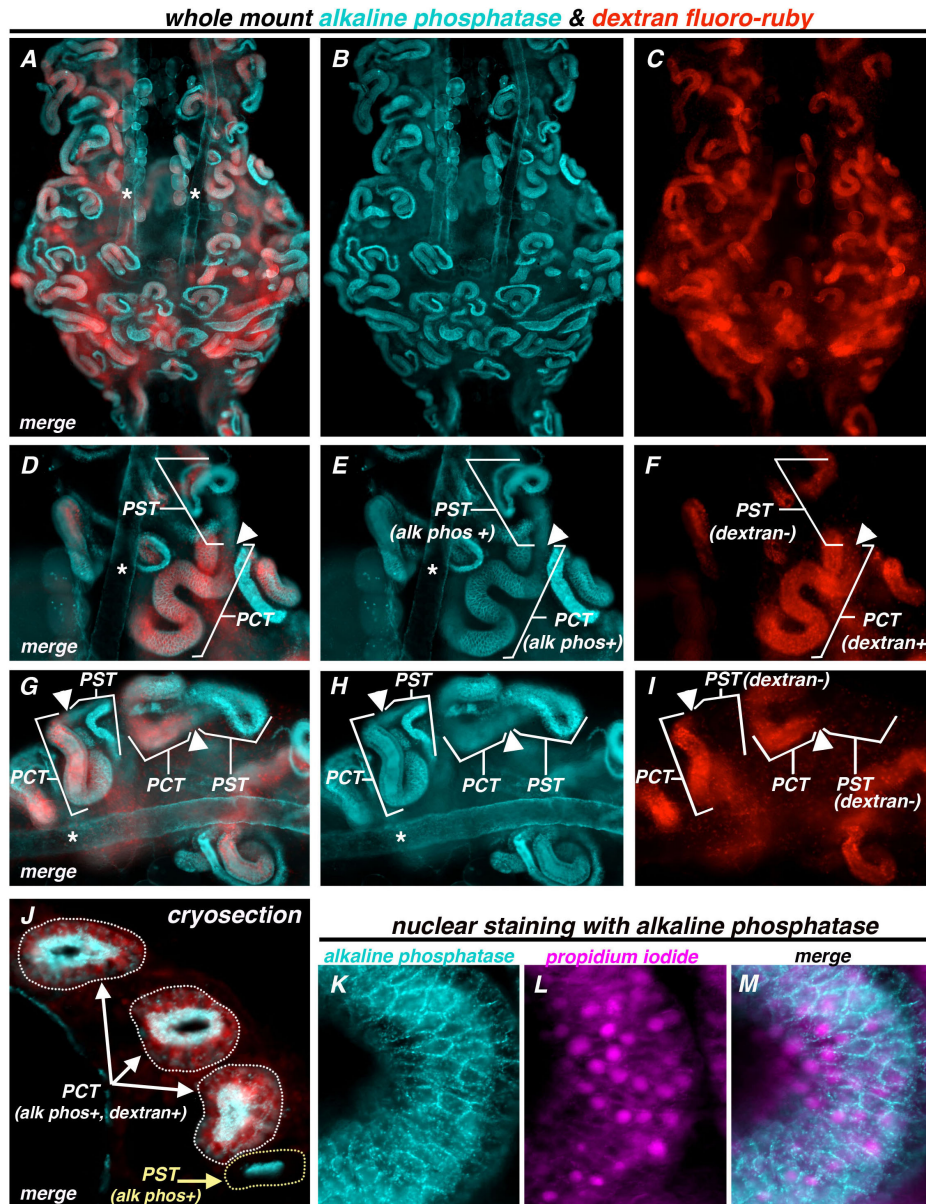


**Figure 6. Alkaline phosphatase and dextran uptake show overlap in the PCT segment of adult kidney nephrons, and alkaline phosphatase staining is compatible with nuclear co-labeling with propidium iodide. (A-I)** Whole mount preparations of alkaline phosphatase staining performed on kidneys from zebrafish adults that had previously received an intraperitoneal injection of dextran fluoro-ruby. Alkaline phosphatase (turquoise) and dextran fluoro-ruby (red) show overlap in the PCT, but not in the PST, which is only positive for alkaline phosphatase. Background levels of alkaline phosphatase illuminate the pair of major collecting ducts in each kidney (asterisks, \*), which are distinctive due to their wide diameter. **(A-C)** Merged image and separate images of the saddle region of a single kidney. **(D-F)** and **(G-I)** Two sets of merged images and separate images of example nephrons. **(I)** Cryosection analysis confirms co-labeling of alkaline phosphatase and dextran fluoro-ruby in PCT segments (outlined in white dots), whereas alkaline phosphatase alone labels the PST segment (outlined in yellow dots). **(K-M)** A kidney was labeled with **(K)** alkaline phosphatase (turquoise) and **(L)** propidium iodide (purple), enabling the **(M)** merged visualization of proximal tubule cells and their nuclei, respectively. [Please click here to view a larger version of this figure.](#)

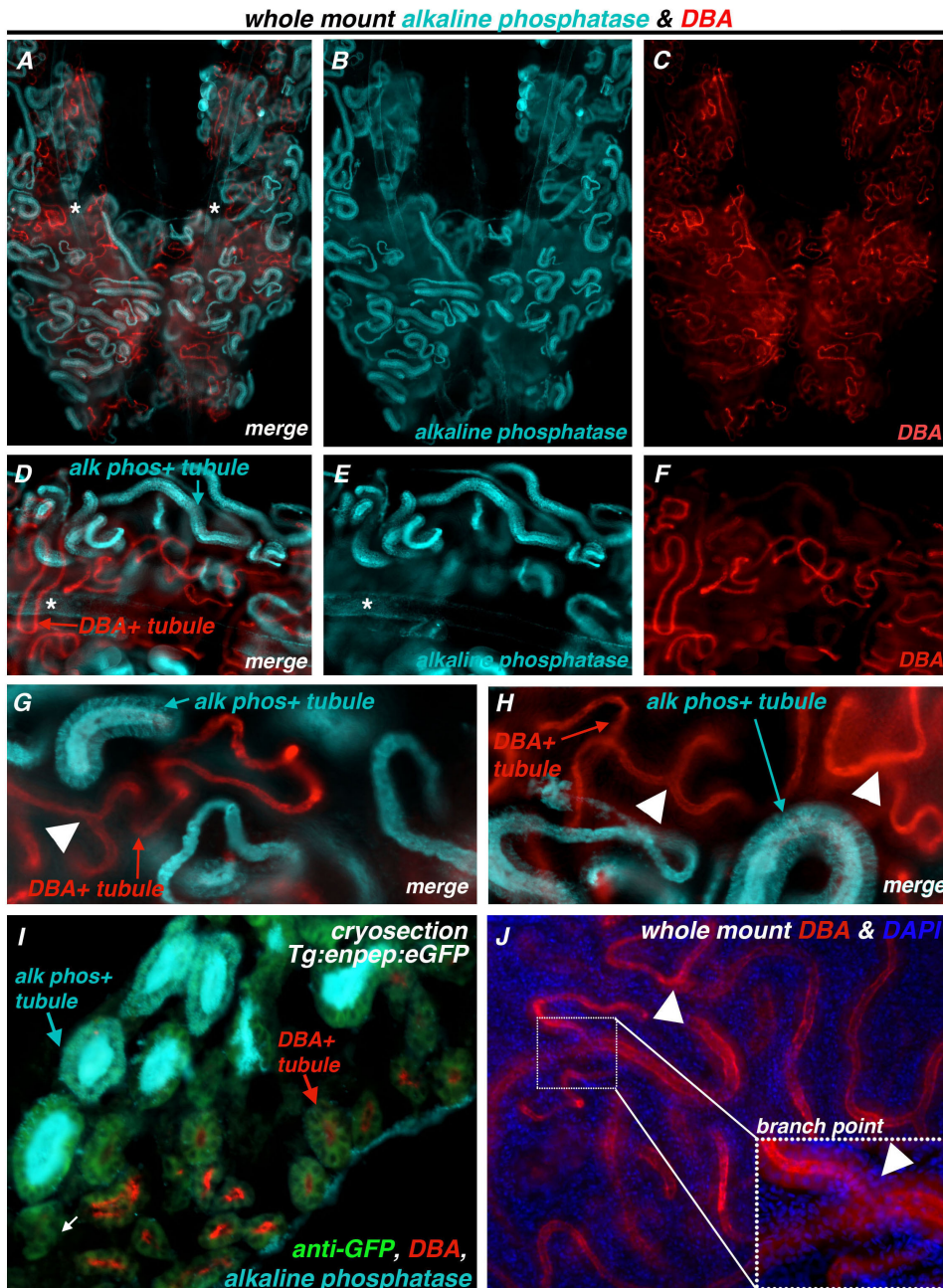


**Figure 7. Alkaline phosphatase and DBA are mutually exclusive segment labels that mark the pan-proximal and pan-distal regions, respectively, present in adult zebrafish kidney nephrons. (A-H)** Whole mount preparations of a zebrafish kidney stained with alkaline phosphatase and rhodamine-DBA. Alkaline phosphatase (turquoise) and DBA (red) do not show overlap in the kidney. Background levels of alkaline phosphatase illuminate the pair of major collecting ducts in each kidney (asterisks, \*), which are distinctive due to their wide diameter. DBA positive tubules are thinner in diameter and characterized frequently by the presence of branch points (white arrowheads). **(A-C)** Merged image and separate images of the saddle region of a single kidney. **(D-F)** One set of merged images and separate images of example nephrons. **(G, H)** Additional examples, with branched DBA tubules alongside alkaline phosphatase positive tubules, merged images. **(I)** Cryosection analysis confirms that alkaline phosphatase and DBA label distinct tubule sections, and only rare tubules show neither label (white arrow), likely due to the angle of section for that tubule. For this analysis, wildtype transgenic fish, *Tg:enpep:eGFP*, were used and all of the renal tubules in this kidney were immunolabeled with a primary antibody to detect GFP. **(J)** Whole mount kidney staining for DBA (red) and DAPI (blue) (merged image), again showing the branched distal tubule segments of the adult nephrons (white arrowhead). [Please click here to view a larger version of this figure.](#)

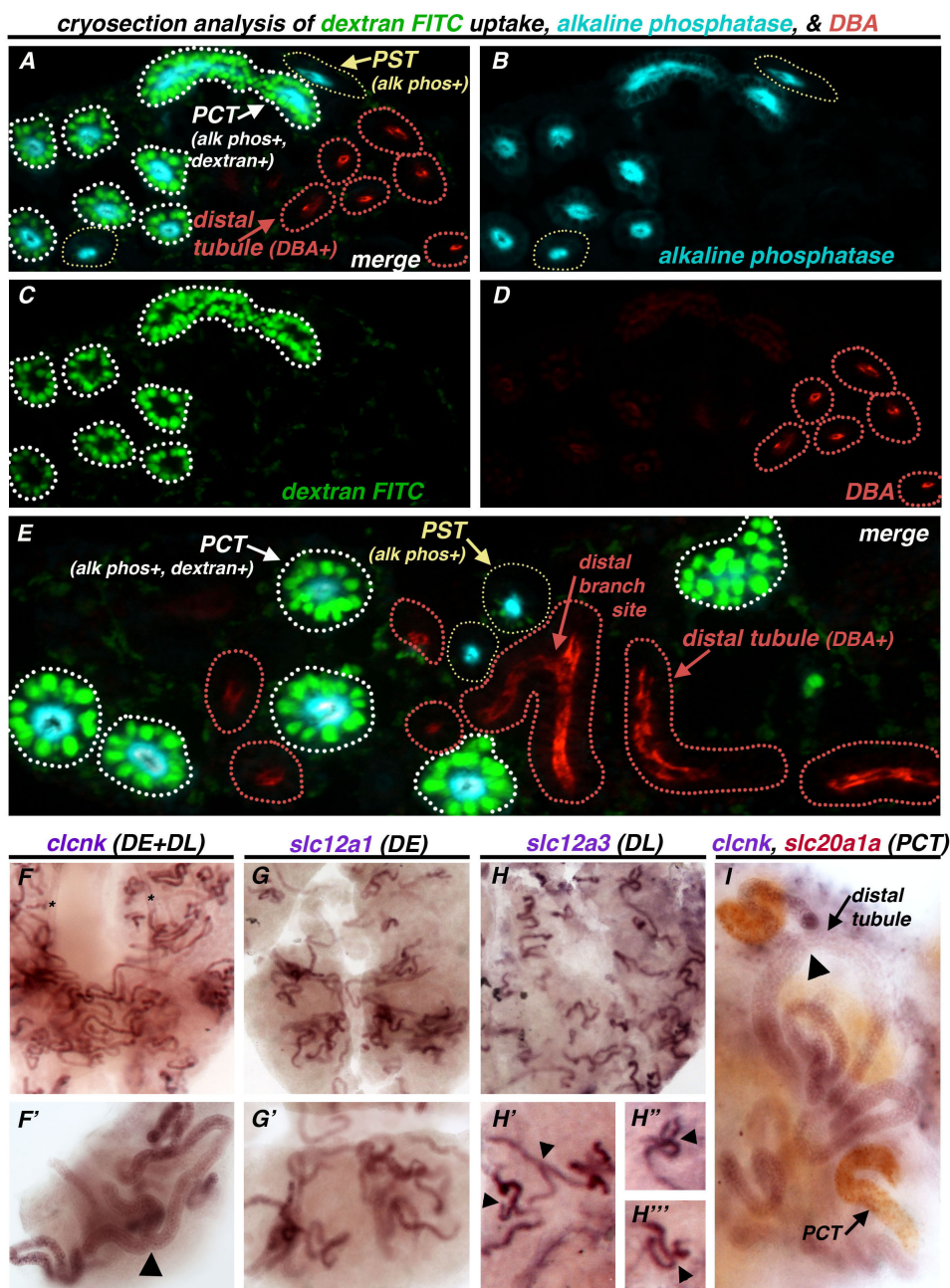


**Figure 8. Triple labeling of adult kidney cryosections with dextran uptake, alkaline phosphatase, and DBA compared to distal segment WISH analysis. (A-E)** Adult kidneys were intraperitoneally injected with dextran-FITC (green), and the kidneys collected 3 days later for embedding and cryosectioning. Staining with alkaline phosphatase (turquoise) and DBA (red) revealed three populations of tubules: PCT segments that were positive for alkaline phosphatase reactivity and dextran (outlined in white dots), PST segments that were positive only for alkaline phosphatase reactivity (outlined in yellow dots), and distal tubule segments that were positive for DBA only (outlined in red dots) which also showed characteristic distal branch points. **(A-D)** Merged image and separate images of one example section. **(E)** Merged image of another example section. **(F-I)** Comparison of distal tubule gene expression patterns by single **(F-H''')** and double **(I)** WISH. The **(F-H')** Single WISH for the listed genes (each in purple staining). **(F,F')** The expression pattern of *clcnk*, a pan-distal (DE-DL) marker, was detected in thin tubules that contained branch points (black arrowhead). **(G,G')** In comparison, WISH for *slc12a1* marks the DE with no branch points detected, and **(H-H''')** *slc12a3* marks the DL, a segment characterized by numerous branch points throughout the kidney organ (black arrowheads). **(I)** Double WISH for the PCT marker *slc20a1a* (red) and the pan-distal *clcnk* (purple). The segments labeled by these markers do not overlap, and rather their expression domains occupy non-adjacent positions, such that individual PCT coils (bottom right) do not abut distal tubules, and the latter occupy discrete locations and possess hallmark branch points (black arrowhead). [Please click here to view a larger version of this figure.](#)

## Discussion

Here, we have described methods that enable the visualization of nephron segment components in the adult zebrafish. The injection of fluorescent dextran conjugates enables preferential PCT labeling due to the endocytic properties of these proximal tubule cells<sup>30,38</sup>. This method

can be performed with great flexibility due to the existence of dextrans that can be obtained with a bevy of different fluorescent conjugates. In addition, the use of lysine-fixable dextrans is an especially convenient way to label PCT segments, as secondary labeling procedures are not required. This enables relatively straightforward signal detection and is compatible with many other fluorescent labels, immunolabeling, and use of transgenic reporter lines. Alkaline phosphatase labeling also marks the proximal tubule, with strong reactivity in the PCT and slightly weaker reactivity in the PST. Finally, the DBA staining enables labeling of distal tubule segments, which display a characteristic branched morphology. Various lectin molecules, which are sugar-binding proteins of nonimmune origin, have been used extensively to distinguish mammalian nephron segments<sup>47</sup>. It is interesting that DBA in the zebrafish correlates with distal tubule segments, as it is utilized to mark collecting ducts in mammalian kidneys<sup>47</sup>.

Taken together, these methods can be utilized in various combinations to document renal composition and function. Since all of these methods can be used in whole kidney preparations, they provide tools to evaluate nephron structure and function throughout the organ without entirely relying on the use of more time-consuming, tedious methods, e.g., cryosection work and immunolabeling. However, the stains described in this methods article are viable in cryosection. Cryosection analysis generates samples (compared to whole mount) that are better suited for immunohistochemistry to detect specific peptides, though of course this type of analysis requires the availability of appropriate primary antibodies. Unfortunately one major limitation in working with the zebrafish animal model remains the poor availability of antibodies. Thus WISH remains the most widely used, i.e., 'go-to,' procedure for the analysis of gene expression. WISH using BCIP, NBT, and/or INT substrate reactions to produce purple or red precipitates is not compatible with fluorescent staining on cryosections. One option would be to invoke the use of fluorescent WISH detection, a procedure that has been optimized for zebrafish embryonic samples and could be tailored for use with the adult kidney. The description of the methods in this video article should allow for further experimentation with techniques like fluorescent WISH in combination with transgenic zebrafish lines in which individual segments are labeled with a reporter such as eGFP or mCherry. Alternatively, the methods described here could be tested in combination with other vital dyes, e.g., other lectins. Thus, further adaptation and expansion of the methods described here could be invoked to suit the researcher's needs for whole mount kidney preparations and analysis.

As such, these methods have broad potential for implementation with the zebrafish model for ongoing regeneration studies and also in genetic disease modeling. There is a pressing need for innovative research and treatments for renal afflictions. Millions of people suffer from some form of kidney disease each year that results from congenital, acute, and/or chronic causes. Further, the prevalence of kidney disease continues to rise worldwide, making these diseases a global public health issue<sup>14,15</sup>. Treatments such as hemodialysis are available whereby an external dialysis machine serves to rid a patient's blood of metabolic waste if their kidneys are not able to perform this role. Unfortunately, this intervention has limitations, as ongoing treatment is necessary for survival. Moreover, patients will eventually require a kidney transplant, which can take years to receive once a patient is placed on a waitlist. Even after obtaining a kidney transplant, many patients suffer adverse effects as a result of the procedure and must battle these effects for the rest of their lives. These difficulties demonstrate the serious need for the development of novel treatments to either help prevent kidney disease or to perhaps augment tissue regeneration<sup>8,16,52,53</sup>. Given the obvious ethical limitations of the use of human test subjects in biomedical laboratories, animal models are essential for the study of human disease pathogenesis and for the testing of new treatments. As a result of its anatomical similarity and evolutionary proximity, the mouse has become the most widely used model of human disease<sup>45</sup>. However, there are certain limitations with this animal, including inability to visualize organ development *in vivo* and practicality of completing large-scale genetic screens. Zebrafish are a relevant and useful model organism for the study of organ development and modeling of human disease<sup>45,46</sup>. In regards to human disease, functional homologs in zebrafish exist for nearly 70% of all human genes<sup>54,55</sup>.

Recent work has highlighted the utility of zebrafish for many areas of kidney research<sup>31,37,56</sup>. Studies of regeneration and repair in zebrafish after AKI suggest that tubule epithelial regeneration and neonephrogenesis are two processes that occur and overlap throughout the regeneration timeframe<sup>30,37</sup>. The use of an aminoglycoside antibiotic called gentamicin has been utilized as an injury paradigm through which to study the outcomes of AKI in adult zebrafish<sup>29,30,37</sup>. Over an approximately two-week period following injury from gentamicin, the proximal tubules regenerate, and meanwhile new nephrons form throughout the organ<sup>29,30,37</sup>. In general, the mechanisms that regulate epithelial regeneration remain highly controversial. In one proposed mechanism of the repair process, there is the initial acute injury event followed by a sloughing of dead cells into the lumen. Next, there is a series of de-differentiation, proliferation, and migration events, after which new cells differentiate, repopulating the injured basement membrane and restoring function to the injured site. Alternatively, other studies have suggested that replacement cells arise from stem/progenitor cells that reside within nephron tubules. As regards the process of neonephrogenesis in zebrafish, cellular aggregates have been observed following AKI by gentamicin injection<sup>29,30</sup>. These aggregates later mature into new nephrons that plumb into already existing tubules<sup>29,30</sup>. The common thread that unites nephron epithelial regeneration and neonephrogenesis is their sheer mystery factor: at present there are exponentially more questions about how these regenerative feats occur than there are available insights.

To date, however, several exciting lines of evidence support the notion that renal regeneration research using zebrafish can indeed provide relevant comparative insights into human AKI that may also have direct translational potential<sup>56-58</sup>. Chemical screening to identify small molecules that increase the proliferation of renal progenitor cells in the zebrafish embryo recently led to the identification of the histone deacetylase inhibitor methyl-4-(phenylthio)-butanoate (m4PTB)<sup>56,57</sup>. Administration of this compound to zebrafish larvae with gentamicin-induced AKI revealed that larval survival increased and that renal tubular proliferation was enhanced<sup>56,58</sup>. When mice with moderate ischemia-induced AKI were treated with m4PTB, their recovery was accelerated in association with a reduction in both tubular atrophy and cell cycle arrest of proliferating renal tubular cells<sup>58</sup>. These findings suggest that the pathways responsible for normal zebrafish renal development and/or the regenerative response to AKI will be conserved with mammals<sup>56</sup>.

Thus, while further studies are needed to tease apart the mechanisms of regeneration—namely to identify the signaling pathways that are involved and understand their interactions—the zebrafish provides one promising avenue to pursue this important goal in the nephrology field. Tools such as the nephron cell labels described in this protocol represent one group of assays that can be utilized to evaluate renal composition and functionality in AKI models. Further, they can be applied to characterize transgenic models of kidney disease and may provide ways to identify chemical therapeutics capable of promoting restoration of nephron structure after renal damage.

## Disclosures

The authors have nothing to disclose.

## Acknowledgements

This work was supported by funding to RAW from the following: National Institutes of Health grants K01 DK083512, DP2 OD008470, and R01 DK100237; March of Dimes Basil O'Connor Starter Scholar grant award #5-FY12-75; start up funds from the University of Notre Dame College of Science and Department of Biological Sciences; and a generous gift to the University of Notre Dame from Elizabeth and Michael Gallagher on behalf of the Gallagher Family to foster stem cell research. The funders had no role in the study design, data collection and analysis, decision to publish, or preparation of the manuscript. We thank the staffs of the Department of Biological Sciences for their support, and the Center for Zebrafish Research at Notre Dame for their outstanding dedication in the care and welfare of our zebrafish colony. Finally, we thank the members of our research lab for their comments, discussions and insights about this work.

## References

1. Reilly, R.F., Bulger, R.E., Kriz, W. Structural-functional relationships in the kidney. In: Schrier RW, ed. *Diseases of the Kidney and Urinary Tract*. Philadelphia, PA: Lippincott Williams & Wilkins; 2-53, (2007).
2. Dressler, G.R. The cellular basis of kidney development. *Annu Rev Cell Dev Biol*. **22**, 509-529, (2006).
3. Nyengaard, J.R., Bendtsen, T.F. Glomerular number and size in relation to age, kidney weight, and body surface in normal man. *Anat Rec*. **232**, 194-201, (1992).
4. Cebrian, C., Borodo, K., Charles, N., Herzlinger, D.A. Morphometric index of the developing murine kidney. *Dev Dyn*. **231**, 601-608, (2004).
5. Schedl, A. Renal abnormalities and their developmental origin. *Nat Rev Genet*. **8**, 791-802, (2007).
6. Ricci, Z., Cruz, D.N., Ronco, C. Classification and staging of acute kidney injury: beyond the RIFLE and AKIN criteria. *Nat Rev Nephrol*. **7**, 201-208, (2011).
7. Faubel, S., et al. Ongoing clinical trials in AKI. *Clin J Am Soc Nephrol*. **7**, 861-873, (2012).
8. Li, Y., Wingert, R.A. Regenerative medicine for the kidney: stem cell prospects and challenges. *Clin Transl Med*. **2**, 11, (2013).
9. Liu, Y. Cellular and molecular mechanisms of renal fibrosis. *Nat Rev Nephrol*. **7**, 684-696, (2011).
10. Murugan, R., Kellum, J.A. Acute kidney injury: what's the prognosis? *Nat Rev Nephrol*. **7**, 209-217, (2011).
11. Palevsky, P.M. Chronic-on-acute kidney injury. *Kidney Int*. **81**, 430-431, (2012).
12. Chawla, L.S., Kimmel, P.L. Acute kidney injury and chronic kidney disease: an integrated clinical syndrome. *Kidney Int*. **82**, 516-524, (2012).
13. Bucaloiu, I.D., Kirchner, H.L., Norfolk, E.R., Hartle, J.E., Perkins, R.M. Increased risk of death and *de novo* chronic kidney disease following reversible acute kidney injury. *Kidney Int*. **81**, 477-485, (2012).
14. Collins, A.J., et al. System. USRDS 2012 Annual Data Report: Atlas of Chronic Kidney Disease and End-Stage Renal Disease in the United States, (2012) *Lancet*. **365**, 331-340, (2005).
15. Meguid El Nahas, A., Bello, A.K. Chronic kidney disease: the global challenge. *Lancet*. **365**, 331-340, (2005).
16. McCampbell, K.K., Wingert, R.A. Renal stem cells: fact or science fiction? *Biochem J*. **444**, 153-168, (2012).
17. Toback, F. G. Regeneration after acute tubular necrosis. *Kidney Int*. **41**, 226-246, (1992).
18. Thadhani, R., Pascual, M., Bonventre, J.V. Acute renal failure. *N Engl J Med*. **334**, 1448-1460, (1996).
19. Bonventre, J. V. Dedifferentiation and proliferation of surviving epithelial cells in acute renal failure. *J Am Soc Nephrol*. **14**, S55-S61, (2003).
20. Romagnani, P, Kalluri, R. Possible mechanisms of kidney repair. *Fibrogenesis Tissue Repair*. **2**, 3, (2009).
21. Bonventre, J.V., Yang, L. Cellular pathophysiology of ischemic acute kidney injury. *J Clin Invest*. **121**, 4210-4221, (2011).
22. Grgic, I., et al. Targeted proximal tubule injury triggers interstitial fibrosis and glomerulosclerosis. *Kidney Int*. **82**, 172-183, (2012).
23. Reimschuessel, R. A fish model of renal regeneration and development. *ILAR J*. **42**, 285-291, (2001).
24. Reimschuessel, R., Williams, D. Development of new nephrons in adult kidneys following gentamicin-induced nephrotoxicity. *Ren Fail*. **17**, 101-106, (1995).
25. Salice, C.J., Rokous, J.S., Kane, A.S., Reimschuessel, R. New nephron development in goldfish (*Carassius auratus*) kidneys following repeated gentamicin-induced nephrotoxicosis. *Comp Med*. **51**, 56-59, (2001).
26. Augusto, J., Smith, B., Smith, S., Robertson, J., Reimschuessel, R. Gentamicin-induced nephrotoxicity and nephroregeneration in *Oreochromis nilotica*, a tilapia fish. *Dis Aquatic Org*. **26**, 49-58, (1996).
27. Elger, M., et al. Nephrogenesis is induced by partial nephrectomy in the elasmobranch *Leucoraja erinacea*. *J Am Soc Nephrol*. **14**, 1506-1518, (2003).
28. Watanabe, N., et al. Kidney regeneration through nephron neogenesis in medaka. *Develop Growth Differ*. **51**, 135-143, (2009).
29. Zhou, W., Boucher R.C., Bollig F., Englert C., Hildebrandt F. Characterization of mesonephric development and regeneration using transgenic zebrafish. *Am J Physiol Renal Physiol*. **299**, F1040-F1047, (2010).
30. Diep, C.Q., et al. Identification of adult nephron progenitors capable of kidney regeneration in zebrafish. *Nature*. **470**, 95-101, (2011).
31. Gerlach, G.F., Wingert, R.A. Kidney organogenesis in the zebrafish: insights into vertebrate nephrogenesis and regeneration. *Wiley Interdiscip Rev Dev Biol*. **2**, 559-585, (2013).
32. Wingert, R.A., et al. The *cdx* genes and retinoic acid control the positioning and segmentation of the zebrafish pronephros. *PLoS Genet*. **3**, e189, (2007).
33. Wingert, R.A., Davidson, A.J. The zebrafish pronephros: a model to study nephron segmentation. *Kidney Int*. **73**, 1120-1127, (2008).
34. Wingert, R.A., Davidson, A.J. Zebrafish nephrogenesis involves dynamic spatiotemporal expression changes in renal progenitors and essential signals from retinoic acid and *irx3b*. *Dev Dyn*. **240**, 2011-2027, (2011).
35. Li, Y., Cheng, C.N., Verdun, V.A., Wingert, R.A. Zebrafish nephrogenesis is regulated by interactions between retinoic acid, *mecom*, and Notch signaling. *Dev Biol*. **386**, 111-122, (2014).
36. Gerlach, G.F., Schrader, L.N., Wingert, R.A. Dissection of the adult zebrafish kidney. *J Vis Exp*. **54**, (2011).
37. McCampbell, K.K., Wingert, R.A. New tides: using zebrafish to study renal regeneration. *Transl Res*. **163**, 109-122, (2014).
38. Drummond, I.A., et al. Early development of the zebrafish pronephros and analysis of mutations affecting pronephric function. *Development*. **125**, 4655-4667, (1998).
39. Anzenberger, U., et al. Elucidation of megalin/LRP2-dependent endocytic transport processes in the zebrafish pronephros. *J Cell Sci*. **15**, 2127-2137, (2006).

40. Majumdar, A., Drummond, I.A. The zebrafish floating head mutant demonstrates podocytes play an important role in directing glomerular differentiation. *Dev Biol.* **222**, 147-157, (2000).
41. Kramer-Zucker, A.G., Wiessner, S., Jensen, A.M., Drummond, I.A. Organization of the pronephric filtration apparatus in zebrafish requires Nephricin, Podocin, and the FERM domain protein Mosaic eyes. *Dev Biol.* **285**, 316-329, (2005).
42. Brien, L.L., Grimaldi, M., Kostun, Z., Wingert, R.A., Selleck, R., Davidson, A.J. Wt1a, Foxc1a, and the Notch mediator Rbpj physically interact and regulate the formation of podocytes in zebrafish. *Dev Biol.* **358**, 318-330, (2011).
43. Ebarasi, L., Oddsson, A., Hultenby, K., Betsholtz, C., Tryggvason, K. Zebrafish: a model system for the study of vertebrate renal development, function, and pathophysiology. *Curr Opin Nephrol Hypertens.* **20**, 416-424, (2011).
44. Swanhart, L.M., Cosentino, C.C., Diep, C.Q., Davidson, A.J., de Caestecker, M., Hukriede, N.A. Zebrafish kidney development: basic science to translational research. *Birth Defects Res C Embryo Today.* **93**, 141-156, (2011).
45. Lieschke, G.J., Currie, P.D. Animal models of human disease: zebrafish swim into view. *Nat Rev Genet.* **8**, 353-367, (2007).
46. Santoriello, C., Zon, L.I. Hooked! Modeling human disease in zebrafish. *J Clin Invest.* **122**, 2337-2343, (2012).
47. Cox, W.G., Singer, V.L. A high-resolution, fluorescence-based method for localization of endogenous alkaline phosphatase activity. *J Histochem Cytochem.* **47**, 1443-1456, (1999).
48. Drummond, I.A., Davidson, A.J. Zebrafish kidney development. *Methods Cell Biol.* **100**: 233-260, (2010).
49. Watson, L., Vassallo, J., Cantor, G., Lehman-McKeeman, L. Lectin histochemistry: an alternative to immunohistochemistry for identify specific structures in rat papillary necrosis. *HistoLogic.* **41**, 28-31, (2008).
50. Cheng, C.N., Li, Y., Marra, A.N., Verdun, V., Wingert, R.A. Flat mount preparation for observation and analysis of zebrafish embryo specimens stained by whole mount *in situ* hybridization. *J Vis Exp.* e51604, (2014).
51. Seiler, C., Pack, M. Transgenic labeling of the zebrafish pronephric duct and tubules using a promoter from the enpep gene. *Gene Expr Patterns.* **11**, 118-121, (2011).
52. Little, M.H. Regrow or repair: potential regenerative therapies for the kidney. *J Am Soc Nephrol.* **17**, 2390-2401, (2006).
53. Romagnani, P., Lasagni, L., Remuzzi, G. Renal progenitors: an evolutionary conserved strategy for kidney regeneration. *Nat Rev Nephrol.* **9**, 137-146, (2013).
54. Goldsmith, J.R., Jobin, C. Think small: zebrafish as a model system of human pathology. *J Biomed Biotechnol.* **2012**, 817341, (2012).
55. Howe, K., *et al.* The zebrafish reference genome sequence and its relationship to the human genome. *Nature.* **496**, 498-503, (2013).
56. Poureetezadi, S.J., Wingert, R.A. Congenital and acute kidney disease: translational research insights from zebrafish chemical genetics. *General Med.* **1**, (3), (2013).
57. Groh, E.D., *et al.* Inhibition of histone deacetylase expands the renal progenitor population. *J Am Soc Nephrol.* **21**, 794-802, (2010).
58. Cosentino, C.C., *et al.* Histone deacetylase inhibitor enhances recovery after AKI. *J Am Soc Nephrol.* **24**, 943-953, (2013).